Spiking patterns emerging from wave instabilities in a one-dimensional neural lattice

V. B. Kazantsev* and V. I. Nekorkin
Institute of Applied Physics of RAS, 46 Uljanov strasse, 603950 Nizhny Novgorod, Russia

S. Binczak and J. M. Bilbault
Laboratoire LE2I, Aile des Sciences de l'ingénieur, Université de Bourgogne, Boîte Postale 47870, 21078 Dijon Cedex, France
(Received 5 June 2002; revised manuscript received 5 May 2003; published 8 July 2003)

The dynamics of a one-dimensional lattice (chain) of electrically coupled neurons modeled by the FitzHugh-Nagumo excitable system with modified nonlinearity is investigated. We have found that for certain conditions the lattice exhibits a countable set of pulselike wave solutions. The analysis of homoclinic and heteroclinic bifurcations is given. Corresponding bifurcation sets have the shapes of spirals twisting to the same center. The appearance of chaotic spiking patterns emerging from wave instabilities is discussed.

DOI: 10.1103/PhysRevE.68.017201 PACS number(s): 82.40.Bj, 05.45.−a, 87.18.Sn, 89.75.Kd

The propagation of nonlinear excitation in neural assemblies is one of the fundamental problems for understanding information transfer in nervous systems. A single neuron produces an excitation pulse (action potential or spike) that is transmitted to the others by means of synaptic coupling (chemical or electrical) [1,2]. The electrical coupling can be described by a linear resistance, then the neuron assembly can be modeled by an array of nonlinear units with a resistive (diffusive) type of connection. The simplest architecture for studying the excitation transmission may be a one-dimensional (1D) lattice (chain) of "reaction-diffusion" type. Many interesting properties of reaction-diffusion (RD) systems may emerge from complex dynamics of traveling waves. Recent studies have reported that a variety of space-time structures originate from interactions and instabilities of traveling waves including elastic collision and backfiring in nerve fibers [3], self-replication of pulses and fractal patterns in a Gray-Scott model [4], wave emitting fronts and pulse turbulence in chemical reaction of CO oxidation of Pt(110) surface [5], spiral wave breakups modeling fibrillation and arrhythmias [6], complex patterns generated by spatiotemporal intermittency [7], and other space-time phenomena in diverse nonlinear media [2,8–10].

In this paper we report on wave patterns in a 1D lattice of electrically coupled spiking neurons modeled by FitzHugh-Nagumo units with modified excitability [11]. In particular, we assume the existence of three fixed points with definite properties (Fig. 1). At variance with the classical single-point FitzHugh-Nagumo model, this modification provides the certain shape of the excitation threshold given by the saddle separatrix [11–13]. As noted in Ref. [5], the three fixed point local dynamics may yield a complex wave behavior of RD systems. Indeed, by studying homoclinic and heteroclinic orbits in a moving frame we shall show that their bifurcation parameter sets are highly nontrivial representing a set of spirals twisting to a codimension-2 point. Then, we shall discuss how the interplay between unstable traveling waves may lead to fractal-like spiking patterns in the lattice. The dynamics of the N-unit lattice of electrically coupled neurons is described by the following system:

$$\dot{u_j} = f(u_j) - v_j + D(u_{j-1} - 2u_j + u_{j+1}),$$

$$\dot{v_j} = \epsilon[g(u_j) - v_j - I], \qquad j = 1,2,\ldots,N. \tag{1}$$

The u_j variable describes the evolution of the membrane potential of the neuron and v_j describes the dynamics of the outward ionic currents (the recovery variable) [8]. The function f has a cubic shape, $f(u) = u - u^3/3$, and the function g is taken piecewise linear, $g(u) = \alpha u$ if $u < 0$ and $g(u) = \beta u$ if $u \geqslant 0$. The parameters α and β control the shape and the location of the v nullcline, hence the exitation threshold. The parameter ϵ defines the time scale of the excitation pulse and the parameter I is a constant stimulus. The dynamics of the single neuron [$D = 0$ in Eq. (1)] is illustrated in phase plane (Fig. 1). The parameters are taken to provide the existence of three fixed points $O_1(u^{(1)},v^{(1)})$, $O_2(u^{(2)},v^{(2)})$, and $O_3(u^{(3)},v^{(3)})$. The points O_1 and O_3 are stable and unstable foci, respectively, the point O_2 is a saddle with the incoming separatrix defining the excitation threshold. Then, if a perturbation of the rest state O_1 is large enough, i.e., lies below the separatrix, the system responds with an excitation pulse, otherwise it decays to the stable rest point O_1 (Fig. 1). Note that the modified FitzHugh-Nagumo unit of network (1) can be

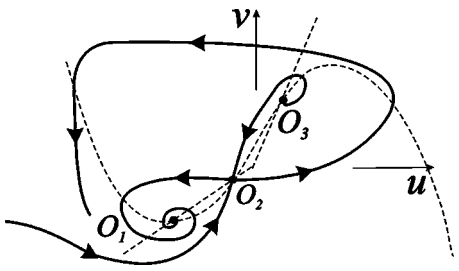

FIG. 1. A qualitative view of the phase plane of the neuron model with modified excitability. Units are arbitrary.

*Electronic address: vkazan@neuron.appl.sci-nnov.ru

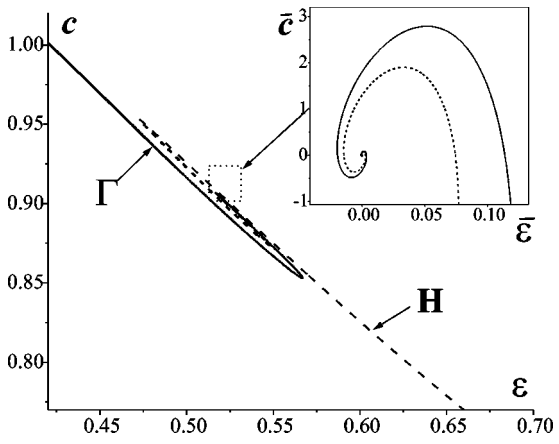

FIG. 2. Bifurcation curves for homoclinic (solid curve) and heteroclinic (dashed curve) bifurcations. The enlarged picture shows the curves near the center of the spiral in the coordinate system: $\bar{\epsilon}=226(\epsilon-\epsilon^*)+219(c-c^*)$, $\bar{c}=-219(\epsilon-\epsilon^*)+226(c-c^*)$. Parameter values: $\alpha=0.5$, $\beta=2$, $I=0.2$, $D=1$. Units are arbitrary.

implemented with an analog electronic circuit [14] and display a required excitable behavior (Fig. 1) in a certain range of experimental parameters.

Let us look for a steadily translating solution of Eqs. (1) in the form $u_j(t)=u(\xi), v_j(t)=v(\xi)$ with $\xi=t-j/c$ being the coordinate moving with the velocity c. Then, in the long-wave approximation from Eqs. (1) we obtain the following ordinary differential equation system:

$$\dot{u}=y,$$

$$\dot{y}=k(y-f(u)+v),$$

$$\dot{v}=\epsilon(g(u)-v-I), \tag{2}$$

where the dot denotes differentiation with respect to ξ and $k=c^2/D$. System (2) has three fixed points $O_1(u^{(1)},0,v^{(1)})$, $O_2(u^{(2)},0,v^{(2)})$, and $O_3(u^{(3)},0,v^{(3)})$. Points O_1 and O_3 are the saddle foci with two-dimensional stable manifold and one-dimensional unstable manifold. The fixed point O_2 has one-dimensional stable manifold and two-dimensional unstable manifold.

To define excitation pulses propagating along the rest state O_1, we search for homoclinic orbits with respect to the fixed point O_1. They represent nontrivial trajectories that asymptotically approach the fixed point with $\xi\to\pm\infty$. In the parameter space of system (2), these correspond to bifurcation of codimension 1. The bifurcation curve calculated numerically in the parameter plane (c,ϵ) is shown in Fig. 2 (solid curve). The curve represents a spiral with focus point (ϵ^*,c^*). For our choice of the parameters: $\epsilon^*=0.522\,760\,187$ and $c^*=0.900\,411\,224$. In the calculations we have observed up to five rotations of the curve. Then, for $\epsilon=\epsilon^*$ there exists a countable number of possible excitation pulses traveling with velocities accounted by the intersections with the spiral curve. The profiles of the homoclinic orbits, hence the profiles of traveling waves, at each turn of the spiral become more and more complicated. Approaching the center of the spiral, the orbits display an increasing number of rotations in the neighborhood of the fixed point O_2. The profiles calculated numerically at the lower turn and near the center are illustrated in Figs. 3(a) and 3(b), respectively. Note that the closer the parameters are to the center, the longer time the trajectory spends in the neighborhood of point O_2. This fact indicates the existence of a heteroclinic contour (cycle) in the phase space of system (2), corresponding to the center of the spiral and to the bifurcation of codimension 2 (Fig. 4). The contour is formed by a common one-dimensional manifold of the points O_1 and O_2 and by a robust intersection of their two-dimensional manifolds [15,16]. Note that the saddle value σ of the saddle focus O_1, $\sigma=\lambda(O_1)+h(O_1)$, where $\lambda(O_1)>0$ is its real eigenvalue and $h(O_1)<0$ is the real part of the complex pair, takes positive values for parameters of the bifurcation curve. Then,

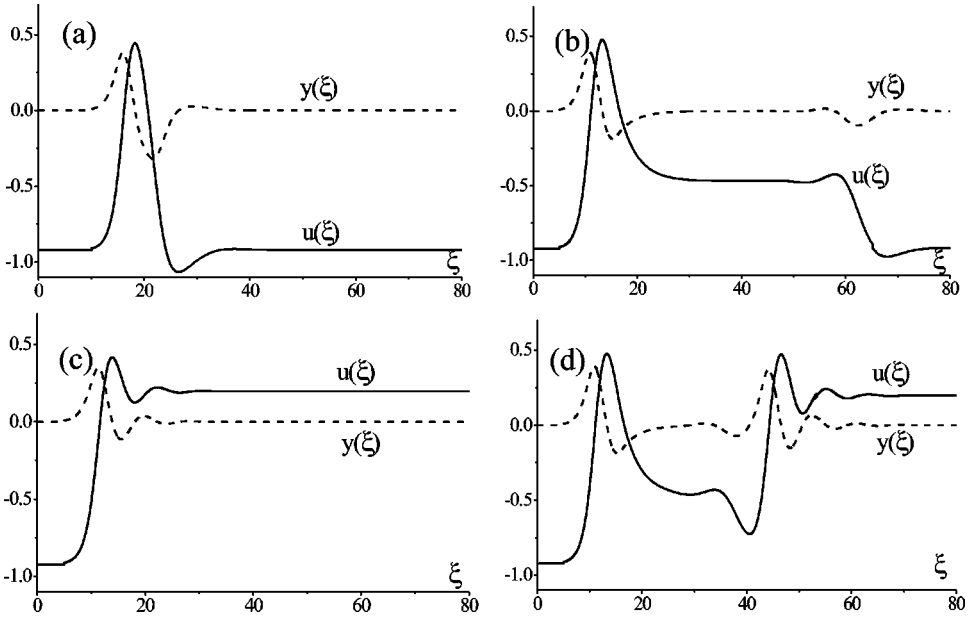

FIG. 3. The profiles $u(\xi)$ and $y(\xi)$ of various homoclinic and heteroclinic orbits. Parameter values: $\alpha=0.5$, $\beta=2$, $I=0.2$, $D=1$, $\epsilon=\epsilon^*=0.52276$. (a) $c=0.893$, (b) $c=0.90041$, (c) $c=0.902$, (d) $c=0.900\,42$. Units are arbitrary.

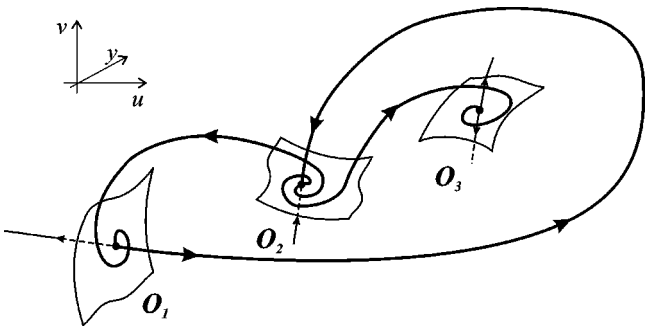

FIG. 4. A qualitative view of the phase space of system (2) for $(\epsilon=\epsilon^*, c=c^*)$. The heteroclinic cycles. Units are arbitrary.

according to the Shilnikov theorem [15], there exists a countable set of saddle periodic orbits and multiloop homoclinic solutions in the neighborhood of the homoclinic bifurcation. It ensures the existence of complex multihump profiles with an arbitrary number of humps. Note that similar codimension-2 contours have been observed in other RD systems with a three-point kinetics [5].

Let us now search for wave fronts or traveling interfaces between the rest state O_1 and the excited state O_3. In terms of Eqs. (2), such solutions are defined by heteroclinic orbits ''linking'' the fixed points O_1 and O_3. Such an orbit represents a trajectory that simultaneously belongs to the unstable manifold of O_1 (approaching O_1 with $\xi\to-\infty$) and to the stable manifold of O_3 (approaching O_3 with $\xi\to+\infty$) in the phase space of system (2). Indeed, such orbits also exist. The interesting fact is that their bifurcation set represents a similar spiral curve twisting to the same center as for homoclinic bifurcation (Fig. 2, dashed curve). It corresponds to another heteroclinic contour existing at the point (ϵ^*, c^*) (Fig. 4). This contour is formed by a common one-dimensional manifold of the points O_1 and O_2 and by the trajectory on the robust intersection of the two-dimensional manifolds of the points O_2 and O_3. Similarly, at each turn of the spiral the number of oscillations of the trajectory near the fixed point O_2 increases, and by approaching the center the time spent in its neighborhood tends to infinity. Typical profiles of the heteroclinic orbits taken from the upper turn of the bifurcation curve and near the center are illustrated in Figs. 3(c) and 3(d), respectively. Therefore, for $\epsilon=\epsilon^*$ system (1) has a countable set of wave front solutions, steadily translating with velocities corresponding to the intersections with the spiral bifurcation curve.

To study wave stability let us check the stability of the three spatially homogeneous steady states, $O_i(u_j(t)=u^{(n)}, v_j(t)=v^{(n)})$, $n=1,2,3$, whose coordinates are defined by corresponding fixed points of the local system (Fig. 1). Solving the linear stability problem for the perturbations of the form $u-u^{(n)}, v-v^{(n)}\sim e^{pt+i\theta j}$ we obtain from Eq. (1) the following dispersion relation:

$$p^2+[\epsilon-f'(u^{(n)})+4D\sin^2(\theta/2)]+\epsilon[D\sin^2(\theta/2)+g'(u^{(n)})-f'(u^{(n)})]=0.$$

It is easy to show that the steady state O_2 is always unstable, and the stability condition for states O_1 and O_3 is $\epsilon>\epsilon^*_{1,3}=f'(u^{1,3})$, respectively. For our choice of the parameters, $\epsilon^*_1\approx0.15$ and $\epsilon^*_3\approx0.96$. Then, the two spiral bifurcation sets shown in Fig. 2 are located between ϵ^*_1 and ϵ^*_3. In this region, the rest state of the chain, O_1, is stable and the excited state O_3 is unstable. The latter ensures the instability of all the wave fronts. It leads to wave emitting front (WEF) propagation [5] when the interface emits a periodic sequence of pulses traveling backward (Fig. 5). Note that in numerical simulations we provided sufficiently smooth profiles (more than ten points per a hump) to satisfy the predictions made in the long-wave approximation. Each pulse represents a solitary excitation of the stable rest state O_1 described by the lower branch of the bifurcation spiral [Fig. 3(a)]. Simulations have shown evolution stability of such solutions for $\epsilon<\epsilon_{cr}$, $\epsilon_{cr}\approx0.566$. However, we may expect the instability of the solutions spending a long time near the unstable state O_2 [Fig. 3(b)]. Simulations of Eqs. (1) with the initial conditions corresponding to different homoclinic orbits have shown that, indeed, such solutions are evolutionary unstable. Then, for $\epsilon>\epsilon_{cr}$ the solitary pulses of simple shape [Fig. 3(a)] also lose the stability. For such parameters the trajectory spends more time near the unstable state O_3, hence the pulses become more longer near the top. As a result the system evolves to a wave emitting interface. The existence of a large number of traveling wave solutions and their evolution instability may lead to complex space-time wave patterns (Fig. 6). The pattern is formed by (i) the pulse emitting fronts (WEFs) and (ii) pulses that due to the instability may create WEFs. Then, pulses and fronts annihilate in collisions and the units return to the rest state until the next excitation comes. As a result, we obtain a triangularlike pattern in the space-time diagram. Note that there are no stable wave solutions and the pattern appears as an interplay between the evolutionary unstable waves. In other words, the system ''jumps'' from one unstable wave to another. In such interpretation, the dynamics of the network is similar to chaotic attractors of low-dimensional systems. The attractor ''attracts'' the trajectories from outside, while there are no stable trajectories inside. Then, the ''skeleton'' of a chaotic attractor

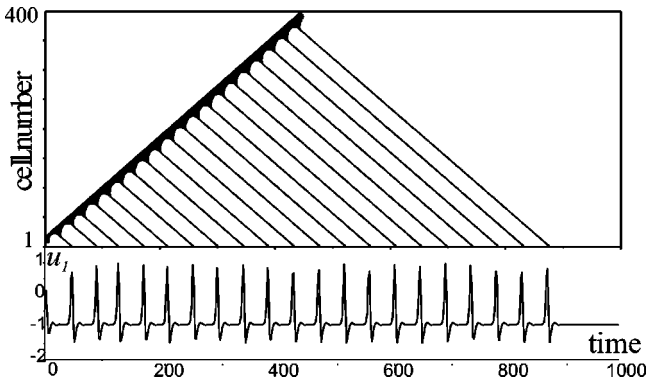

FIG. 5. (a) Wave emitting front (WEF) in the 1D lattice of neurons (1) emerging from wave instabilities for $N=1000$. The interface between black and white colors is drawn at the level $u_j=0$. (b) A spike train at the unit $j=1$ created by the WEF. Parameter values: $\alpha=0.5, \beta=2, I=0.2, \epsilon=0.54, D=1$. Units are arbitrary.

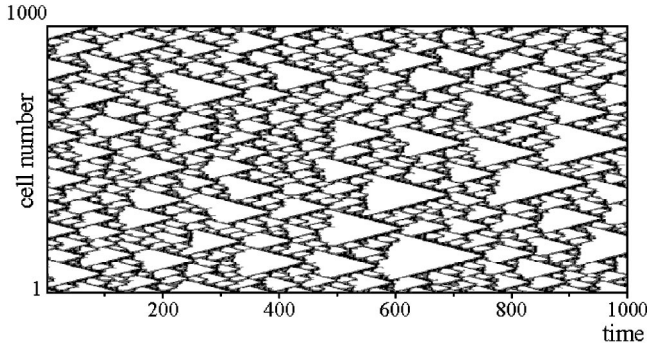

FIG. 6. Spiking pattern in the 1D lattice of neurons (1) emerging from wave instabilities for $N=1000$. Parameter values: $\alpha=0.5$, $\beta=2$, $I=0.2$, $\epsilon=0.57$, $D=0.5$. Units are arbitrary.

is formed by a countable number of unstable or saddle periodic orbits. In the case of Eqs. (1), such a skeleton of a self-sustained space-time pattern is formed by a large number of unstable traveling waves.

The spiking pattern in Fig. 6 displays a self-similarity with multiscale triangles similar to Sierpinsky gaskets created by self-replicating pulses in the Gray-Scott model [4]. The triangles are formed by the unstable pulses and fronts that have about the same velocities (Fig. 2). The fractal dimension of the spike distribution (black points in Fig. 6) in the lattice calculated by box counting method is $D_f=1.73-1.75$. Note that at the single-cell level, each neuronlike unit exhibits a chaotic sequence of spikes (action potentials) resulting with variable interspike intervals [Fig. 7(a)] [17,18]. Its probability distribution for the boundary unit, $j=1$, is shown in Fig. 7(b). There is a nonzero probability to have spikes in a wide range of intervals. Then, the histogram has two maxima. These correspond to the characteristic time scales of the two main instabilities [(i) front (WEF) instability and (ii) pulse instability creating WEF] responsible for the fractal spiking pattern in the neural lattice.

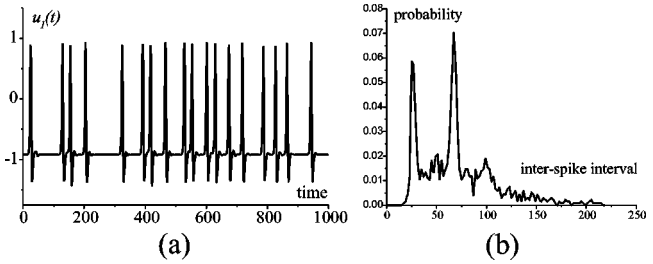

FIG. 7. (a) A spike train at the unit $j=1$ corresponding to the fractal pattern. (b) Interspike interval probability distribution. Units are arbitrary.

We have shown how the 1D neural lattice displays self-sustained spiking patterns emerging from an interplay between unstable nonlinear waves. Such patterns appear without any stimulus and can be treated as an ''eigenstate'' of the neuron assembly. The local oscillations represent chaotic sequences of pulses which, however, are organized in a fractal triangularlike space-time pattern. Note that the interspike interval has two maxima indicating, in essence, the presence of two ''eigenfrequencies'' in the system. In conclusion, we hope that our study will be helpful in understanding the dynamic origin of complex spiking patterns responsible for various information processing functions of the brain.

This research has been supported by the Russian-French program of joint research (Grant No. 04610PA) and the Russian Foundation for Basic Research (Grant Nos. 01-02-17638 and 03-02-17135). V.B.K. acknowledges the financial support from the INTAS (Grant No. YSF 2001-2/24) and the Russian Science Support Foundation. V.I.N. acknowledges the support from the University of Burgundy.

[1] *Principles of Neural Science*, 3rd ed., edited by E.R. Kandel, J.H. Schwartz, and T.M. Jessell (Prentice-Hall, Englewood Cliffs, NJ, 1991).
[2] J.D. Murray, *Mathematical Biology* (Springer-Verlag, Berlin, 1993).
[3] O.V. Aslandi and O.A. Mornev, Mat. Modelirovanie **11**, 3 (1999) [Mathematical Modeling **11**, 3 (1999)].
[4] Y. Hayase, J. Phys. Soc. Jpn. **66**, 2584 (1997); Y. Hayase and T. Ohta, Phys. Rev. Lett. **81**, 1726 (1998); Y. Hayase and T. Ohta, Phys. Rev. E **62**, 5998 (2000).
[5] M.G. Zimmermann *et al.*, Physica D **100**, 92 (1997); J. Krishnan *et al.*, Comput. Methods Appl. Mech. Eng. **170**, 253 (1999); M. Or-Guil *et al.*, Physica D **135**, 154 (2000); M. Or-Guil *et al.*, Phys. Rev. E **64**, 046212 (2001).
[6] A. Karma, Phys. Rev. Lett. **71**, 1103 (1993).
[7] H. Chaté and P. Manneville, Phys. Rev. Lett. **58**, 112 (1987); Physica D **32**, 409 (1988).
[8] A. Scott, *Nonlinear Science: Emergence and Dynamics of Coherent Structures* (Oxford University Press, New York, 1999).
[9] J. Brindley, A.V. Holden, and A. Palmer, in *Nonlinear Wave Processes in Excitable Media*, edited by A.V. Holden *et al.* (Plenum Press, New York, 1991).
[10] K.J. Lee, R.E. Goldstein, and E.C. Cox, Phys. Rev. Lett. **87**, 068101 (2001).
[11] V.B. Kazantsev, Phys. Rev. E **64**, 056210 (2001).
[12] J. Rinzel and B. B. Ermentrout, in *Methods in Neuronal Modelling*, edited by C. Koch and I. Segev (MIT Press, Cambridge, MA, 1998), pp. 251–292.
[13] E.M. Izhikevich, Int. J. Bifurcation Chaos Appl. Sci. Eng. **10**, 1171 (2000); S.P. Dawson, M.V. D'Angelo, and J.E. Pearson, Phys. Lett. A **265**, 346 (2000).
[14] S. Binczak *et al.* Electron. Lett. (to be published).
[15] L.P. Shilnikov *et al.*, *Methods of Qualitative Theory in Nonlinear Dynamics* (World Scientific, Singapore; 1998), Pts. I and II.
[16] V.V. Bukov, Physica D **62**, 290 (1993).
[17] M.C. Eguia, M.I. Rabinovich, and H.D.I. Abarbanel, Phys. Rev. E **62**, 7111 (2000).
[18] N. Brenner *et al.*, Neural Comput. **12**, 1531 (2000).